

RSC Advances



This is an *Accepted Manuscript*, which has been through the Royal Society of Chemistry peer review process and has been accepted for publication.

Accepted Manuscripts are published online shortly after acceptance, before technical editing, formatting and proof reading. Using this free service, authors can make their results available to the community, in citable form, before we publish the edited article. This *Accepted Manuscript* will be replaced by the edited, formatted and paginated article as soon as this is available.

You can find more information about *Accepted Manuscripts* in the [Information for Authors](#).

Please note that technical editing may introduce minor changes to the text and/or graphics, which may alter content. The journal's standard [Terms & Conditions](#) and the [Ethical guidelines](#) still apply. In no event shall the Royal Society of Chemistry be held responsible for any errors or omissions in this *Accepted Manuscript* or any consequences arising from the use of any information it contains.

Chemical Analysis of Primary Combustion Products of Boron-based Fuel-rich Propellant

*Lin-lin Liu**, Guo-qiang He, Ying-hong Wang, Song-qi Hu

Science and Technology on Combustion, Internal Flow and Thermal-Structure

Laboratory, Northwestern Polytechnical University, Xi'an 710072, PR. China

Keywords: boron-based fuel-rich propellant; primary combustion; condensed phase products; chemical analysis

Abstract: A facility was designed to collect the primary combustion products of boron-based fuel-rich propellants under different chamber pressures. Morphology and particle size of condensed phase products were analyzed by laser particle size analyzer and scanning electron microscope (SEM), and the chemical analysis of condensed phase products was carried out by X-ray diffraction (XRD), Laser Raman Spectrometer, wet chemical analysis and element analyzer. In addition, organics in condensed phase products and gases products were analyzed by Fourier Transform Infrared Spectrometer (FTIR) and Gas Chromatography (GC), respectively. The results show that the condensed phase products are mainly consisted of B, C, B₄C, (or B₁₂C₂), BN, Mg, MgO, MgAl₂O₄, Al, Al₂O₃, AlCl₃, NH₄[Mg(H₂O)₆]Cl₃, NH₄Cl and Fe₃O₄; there are large amounts of boron oxide and boron carbide in condensed phase products which indicates elemental boron is highly active during the primary

combustion process; higher chamber pressure may be disadvantageous to the secondary combustion efficiency because more inactive boron carbide, graphite and *h*-BN (especially boron carbide) are produced.

Introduction

Metal Fuels (especially aluminum) are usually added into solid propellants to improve the specific impulse (I_s) of the solid rocket¹, and the energy of boron-based fuel-rich propellants is the highest (can reach more than 35 kJ/g) among all the solid propellants because of the high energy density (58.74 kJ/g or 137.45 kJ/cm³) of boron². Concerning that oxygen consumption of boron per unit mass is much higher than that of aluminum and magnesium, boron could only be employed in case of air-breathing propulsion devices, and this is why boron-based fuel-rich propellant is the most promising energy source for solid fuel ramjet (SFRJ)³⁻⁵.

The combustion of boron-based fuel-rich propellants could be divided into two stages, viz. primary combustion and secondary combustion. Primary combustion depends on the oxidizer in the propellants to support the combustion, and the intermediate products are generated during this process. The secondary combustion takes place when the intermediate products react with the inhaled oxygen from the environment after they are ejected to the secondary combustion chamber. Therefore, the study concerning the primary combustion could provide important information not only for the primary combustion mechanism but also for the study of the secondary combustion^{6,7}.

The primary combustion of boron-based fuel-rich propellants is much more complicated compared with the combustion of normal composite propellants because of the low oxidizer content and the complication of the combustion process of boron particles^{8,9}. As a consequence, there is no effective method to study the mechanisms of the combustion process at present. Since the combustion products could reflect the results of chemical reactions among the ingredients of the propellants, the chemical analysis of the primary combustion products would provide helpful information for the studies concerning the combustion mechanisms.

At present, there are two methods to determine the component of the combustion products, viz. thermodynamics calculation and experimental measurement. Thermodynamics calculation mainly refers to the calculation by minimization of Gibbs free energy and is used most commonly because the results could be obtained easily for any propellants under any combustion conditions (pressure and temperature) theoretically^{10, 11}. However, the calculation results are usually unsatisfactory for the high-metal loading propellants because the chemical reactions among metal fuels and oxidizing gases are much slow and the Gibbs free energy of the system usually cannot reach the minimum which results in the kinetically controlled combustion process. Therefore, although the thermodynamic calculation is convenient to be employed, the calculation results cannot meet the requirement of accuracy¹².

The composition of combustion products is also usually determined by experiments, and there are some studies about boron related combustion products. A closed-type

strand bomb was developed by Mitani and Izumikawa to trap the combustion products of propellants, and the combustion efficiencies of boron was investigated by titration method¹³. But small propellant grain was used in the experiment (a propellant strand with 8 mm in diameter and 20 mm in length) and the combustion products may be different from the fact ones because of the heat losses. In addition, the condensed phase elements were cooled by water and the hot boron particles could react with water which results in the higher combustion efficiencies of boron.

Swirl and fuel composition effects on the combustion of boron in solid-fuel ramjets was studied by Pein and Vinnemeier. The exhaust particle sampling facility was developed by them to collect the condensed phase products, and then the composition of the products were analyzed by Auger Electron Spectroscopy (AES), X-ray Photoelectron Spectroscopy (XPS) and X-ray Diffraction (XRD)^{14, 15}. Although AES and XPS could represent the depth and location profile of combustion products quantitatively and qualitatively, the accuracy of the results is usually not satisfactory because they are all surface analysis techniques. Compared with secondary combustion products, the elements of primary combustion products are more complicated, and quantitative analysis by XRD could almost not be carried out.

At present, there are two issues for the elements determination of primary combustion products of boron-based fuel-rich propellants. The first, it is difficult to collect the combustion products the same as those ejected from the gas generator, the second is,

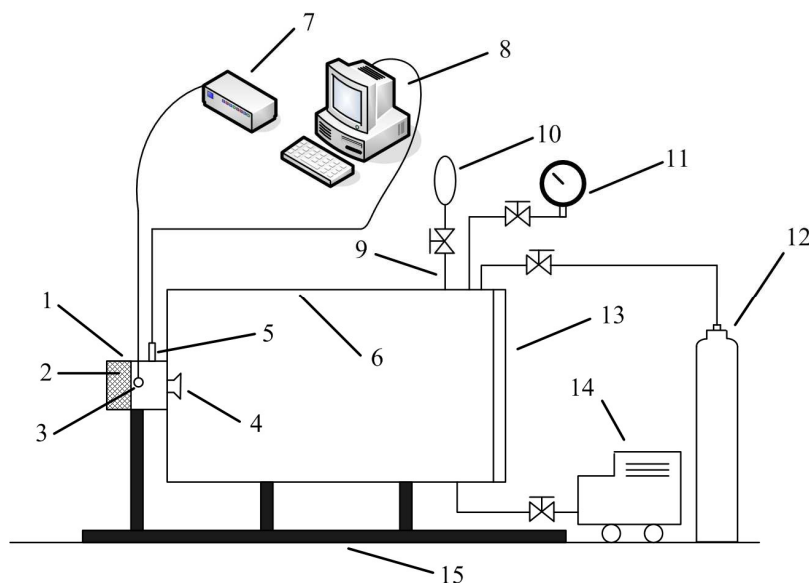
the elements of combustion products are complicated and the chemical analysis is difficult to carry out.

A facility was designed to collect the primary combustion products in this study, and the collected products are almost the same as those ejected from the gas generator by freezing the chemical reactions. In addition, chemical analysis of primary combustion products (especially condensed phase products) was carried out using various methods.

1 Collection of primary combustion products

1.1 Experimental facility

In order to determine the elements of primary products of boron-based fuel-rich propellants, a facility that has capacity to capture all the combustion products must be designed first. Considering that the primary combustion temperature of boron-based fuel-rich propellants is high (usually 1800 K~2000 K) and the component must be analyzed at the room temperature, the combustion products must be cooled before the measurement. Therefore, the reactions among the products must be prevented during the cooling process. A facility was designed in this study to collect the combustion products, and the schematic diagram is shown in Figure.1.



1-gas generator; 2-propellant grain; 3-igniter pad; 4-nozzle; 5-pressure transducer; 6- collection tank; 7-igniter; 8-signal acquisition system; 9-gaseous products collecting piping/gas exhaust piping; 10-teflon bag; 11-vacuum manometer; 12-hyperbaric argon cylinder; 13-the door of collection tank; 14-vacuum pump; 15-holder

Fig. 1 Schematic diagram of the experimental facility

The air was discharged from the collection tank first by pumping vacuum, and then fill argon many times (no less than three times) to prevent the reactions between the combustion products and environment. The propellant grain loaded in the gas generator was ignited, and the collection process was carried out after the combustion products were cooled. The gas sampling bag made of fluorinated ethylene propylene (FEP) with the volume of 50 ml was employed to collect the gaseous products through the gaseous products collecting piping, and the condensed phase products (including solid products and liquid products) were collected after the exhaust. The chamber pressure was measured by the pressure transducer during the ignition and combustion process of the propellant. The condensed phase products were dried at 80 °C under vacuum for 12 hours before the analysis.

The combustion conditions of the propellants in this facility were almost the same as those in the gas generator, and the condensed phase products were widely dispersed in the stainless steel collection tank with large volume (about 2 m³) which would decrease the chemical reactions among the condensed phase products to certain level. The large wall heat transfer would occur after the ejection due to the high thermal conductivity of stainless steel which is also benefit for the cooling of the products. In addition, the collection tank was filled with inert gas (argon) and argon also played an important role in avoiding reactions among the combustion products by increasing the cooling rate and diluting the combustion reactants.

It should be noted that some gaseous products ejected from gas generator, such as NH₃, H₂O, MgCl₂ and HCl may be existed in the form of liquid or solid by physical and chemical interactions among them during the cooling of combustion products. Since the content of boride is the most important among all the primary products and the effect of cooling process on the mass of condensed phase could be eliminated by certain correction, the results of chemical analysis are reliable and can represent the real composition of condensed phase products.

1.2 Collection process

Boron-based fuel-rich propellants were prepared to collect the primary products. The formulation of the propellant is hydroxyl-terminated polybutadiene (HTPB) 19.0 %, dioctyl sebacate (DOS) 4.0 %, Catocene 4.0 %, ammonium perchlorate (AP) 34.0 %, and

boron powder 26.0 %, magnesium powder 7.5 %, aluminum powder 4.0 %, toluene-2,4-diisocyanate (TDI) 1.5 %.

As metal fuel particles are all coated by the film of their oxide and there exists the other impurities in the original metal powder, the content of boron, magnesium and aluminum in their powders was measured to investigate the exact ingredients in the propellant. Boron powder was dissolved in boiling dilute nitric acid first and elemental boron was oxidized to be boric acid (H_3BO_3), and the content of boron in boron powder was measured by acidimetry with mannitol¹⁶. Magnesium powder and aluminum powder were solved in dilute hydrochloric acid, the content of magnesium and aluminum was determined by EDTA complexometric titration of filtrate with xylenol orange and erichrome black T as indicator respectively^{17, 18}. The results show that amount of boron, magnesium and aluminum in the propellant is 25.015 %, 6.986 % and 3.853 % respectively.

A propellant strand (96 mm in diameter and 35 mm in length) was used in the experiments, and the strand was an end-burning grain with the side face and one of the end faces coated by liner (Fig.2). The powder of the same propellant was employed to ignite the propellant grain.



Fig.2 Propellant strand

Chamber pressure is important for the combustion products composition of the propellants. Experiments were carried out three times in this study, and the chamber pressure of each experiment changes by the change of nozzle throat diameter. The experimental conditions and chamber pressures of the experiments are shown in Table 1 and Figure 3.

Table 1 Experimental conditions and experimental results

NO.	Nozzle throat diameter/mm	Maximum pressure / MPa	Average pressure / MPa	Combustion time / s
1	10.00	0.323	0.234	6.044
2	8.00	1.172	0.766	4.922
3	5.00	4.494	3.678	2.832

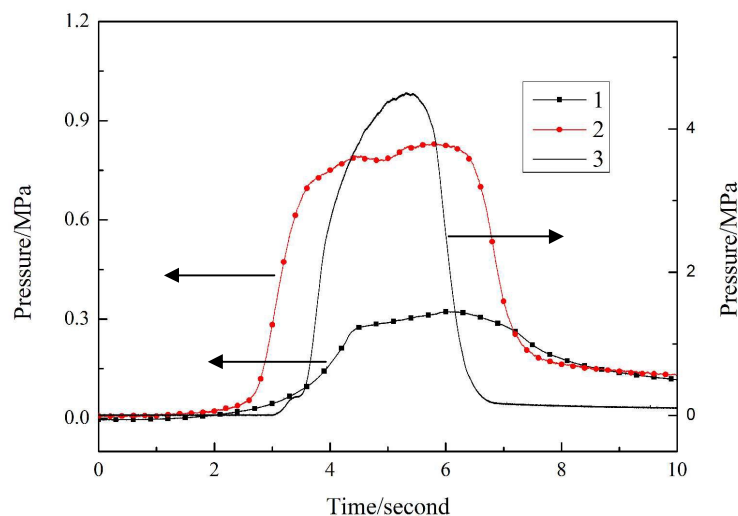


Fig.3 Pressure - time curve of experiments

Figure 3 indicates that the chamber pressure cannot stay almost the same during the combustion process of the propellant which is common in case of small rocket motor. In order to investigate the effect of pressure on the combustion products, time-averaged pressure P_c was used to characterize the operation one.

The pressure curve of the rocket motor could usually be divided into three parts, i.e. start-up phase, steady-state phase and tail-off phase. The steady-state phase clearly dominates the overall performance of the motor, and the chamber pressure is usually calculated by this phase, so the starting point and end point of this phase must be determined.

In the experiment, starting point of steady-state phase t_1 is defined as the time corresponding to the inflection point of pressure during the start-up phase and end point of steady-state phase t_2 is defined as the time corresponding to the inflection point of pressure during the tail-off phase. The time-averaged chamber pressure P_c could be defined by:

$$P_c = \frac{\int_{t_1}^{t_2} p dt}{t_2 - t_1}$$

2 Morphology and particle size of primary condensed phase products

Usually, burning time of solid fuel increases with the particle size, so the particle size of primary condensed phase products plays an important role in the secondary combustion of boron-based fuel-rich propellants. The distribution of condensed phase products in each experiment (named #1, #2 and #3 respectively) was measured by laser particle size analyzer (Mastersizer 2000, Malvern), and the results are shown in Figure 4 and Table 2.

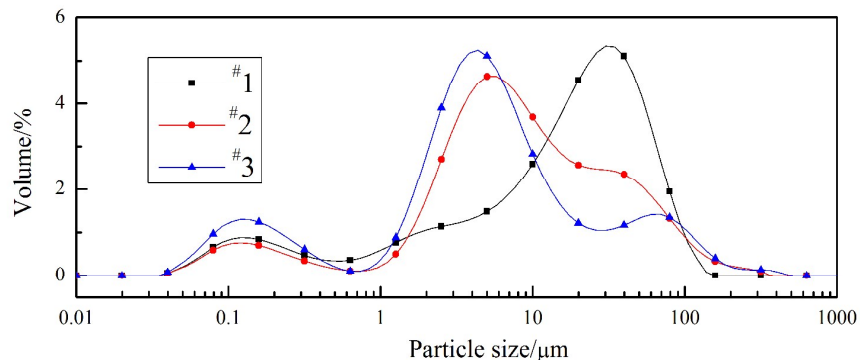


Fig.4 Particle size distribution of condensed phase combustion products

Figure 4 shows that the particle size of #1 sample is mainly in the range of 10~100 μm , but 1~20 μm for the other two samples.

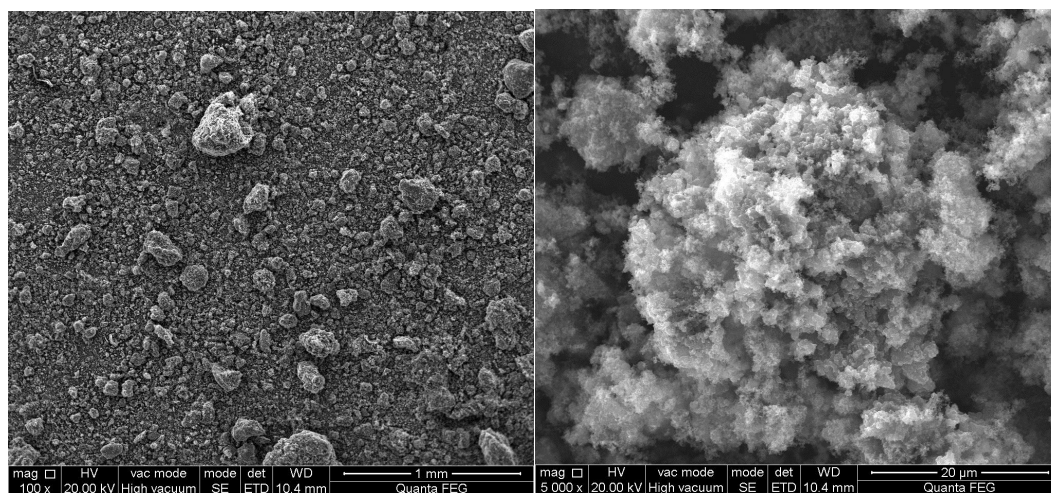
Table 2 Results of particle size distribution

NO.	Pressure/MPa	$d(0.1)/\mu\text{m}$	$d(0.5)/\mu\text{m}$	$d(0.9)/\mu\text{m}$	$D[4,3]/\mu\text{m}$	Uniformity
#1	0.234	0.391	12.124	53.744	22.903	1.56
#2	0.766	0.127	7.103	74.092	18.938	2.21
#3	3.678	0.176	4.429	47.966	16.223	3.23

Figure 4 and Table 2 indicate that the average particle size of all samples is less than 25 μm which means that there is no severe agglomeration between the metal fuel particles during the combustion. The particle size decreases but the uniformity of particle size increases with the increase of chamber pressure basically. More products with larger particle size (more than 100 μm) was produced under high pressure, and the results of energy dispersive spectrometer (EDS), scanning electron microscope (SEM) and X-ray diffraction (XRD) show that they are porous amorphous carbon. Amorphous carbon burns easily during the secondary combustion, and then the large particles do not have adverse effect on the heat release of secondary combustion. So

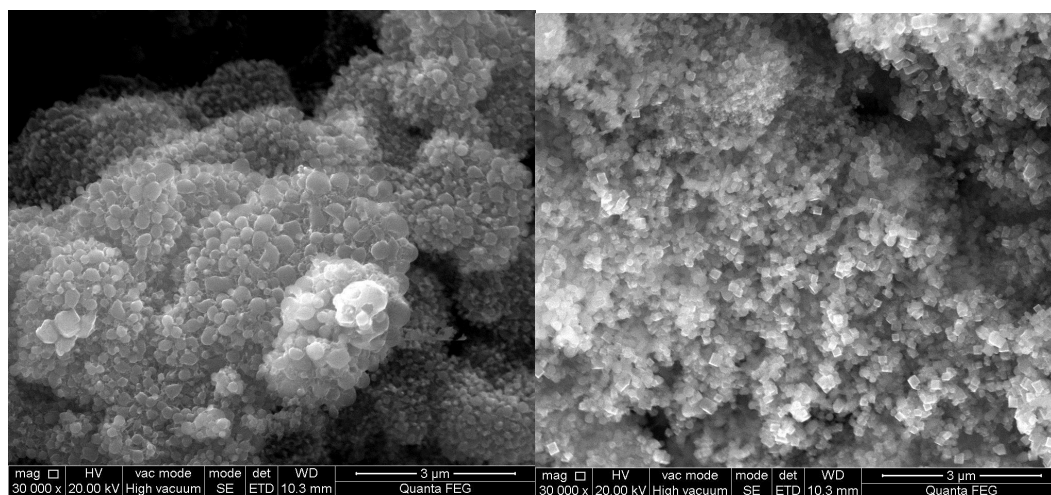
from the standpoint of particle size, the high pressure will facilitate the combustion efficiency of the secondary combustion.

Samples were also characterized by scanning electron microscope (Quanta 600 FEG, FEI), a series of typical SEM graphs with different magnifications are shown in Figure 5.



(a)

(b)



(c)

(d)

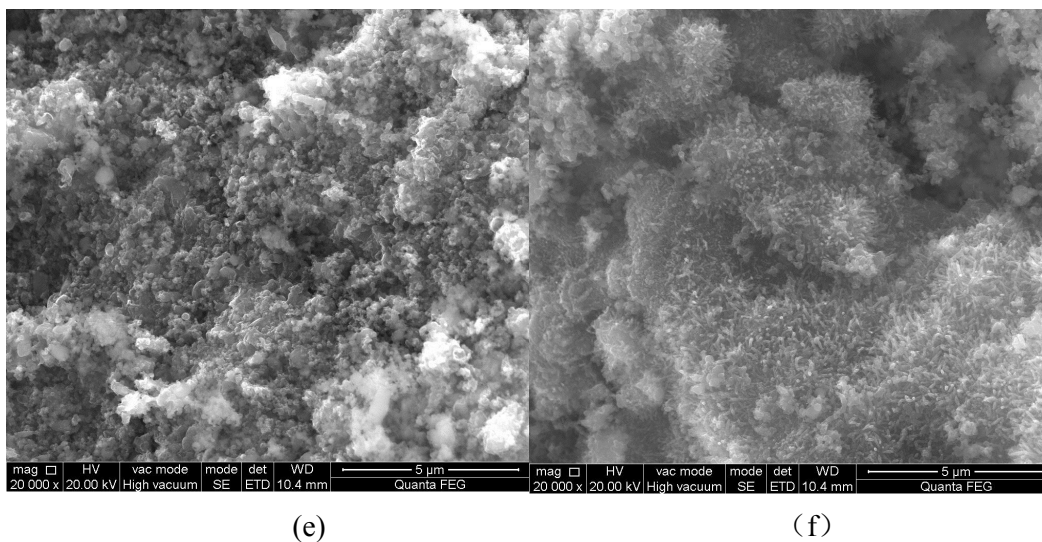


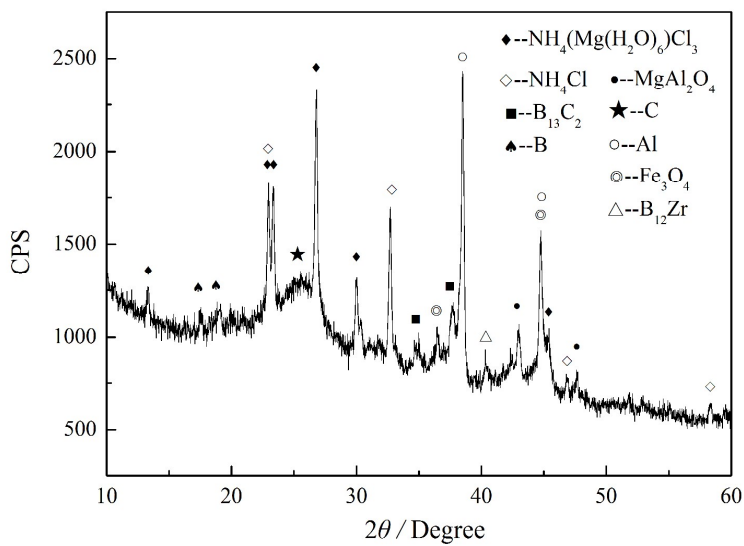
Fig.5 SEM images of condensed phase products

Figure 5(a) also indicates that there are particles with different size in the sample. Figure 5(b) is the enlargement of the large particle in Figure 5(a), and the results of EDS show that it is carbon. In addition, the results of EDS indicate that the substances in Figure 5(c) ~ Figure 5 (f) may be boron carbide, magnesium oxide, unreacted boron and boron oxide respectively.

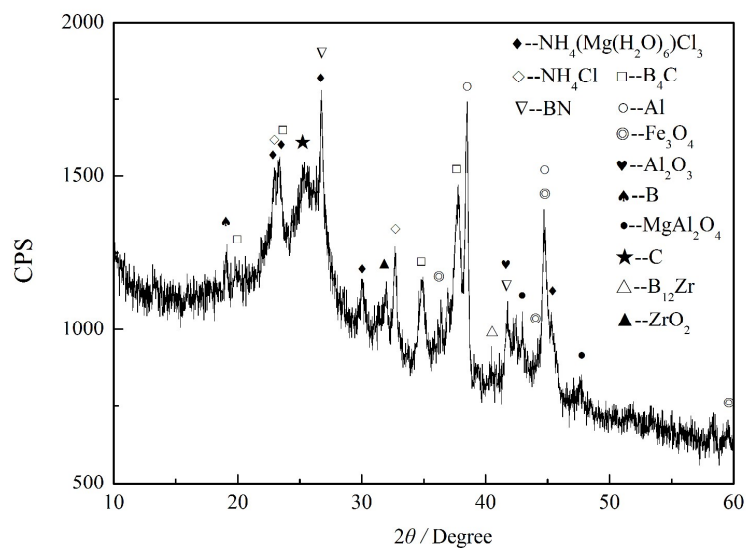
3 Chemical analysis of condensed phase products qualitative and quantitative aspects

3.1 XRD and Raman analysis of the samples

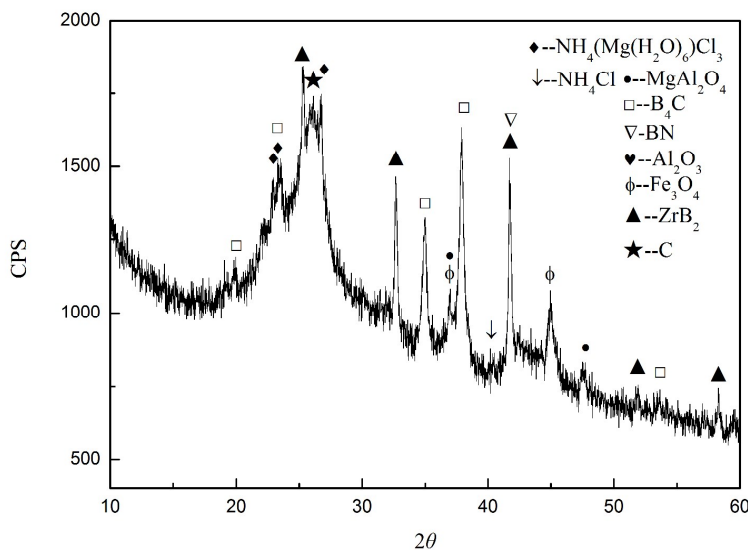
The powder XRD measurements of the samples were recorded on a Bruker D8 Advance X-ray powder diffractometer using Cu K α radiation ($\lambda = 1.5406 \text{ \AA}$) with scattering angles (2θ) of 10-60°, the results are shown in Figure 6.



(a) #1 sample



(b) #2 sample



(c) #3 sample

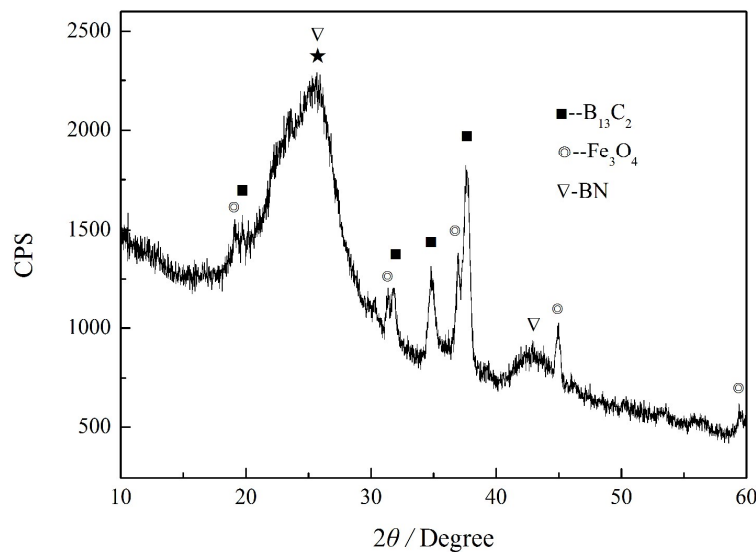
Fig.6 XRD patterns of the samples

Figure 6 suggests that the condensed phase products are mainly consisted of B_4C (or $B_{12}C_2$), B, BN, $NH_4[Mg(H_2O)_6]Cl_3$, NH_4Cl , C, Al, Al_2O_3 , $MgAl_2O_4$, Fe_3O_4 , etc. Chamber pressure affects the elements of condensed phase products, boron carbide exists in the form of $B_{12}C_2$ and there is no Al_2O_3 under low pressure, but boron carbide exists in the form of B_4C and there is no elemental Al under high pressure.

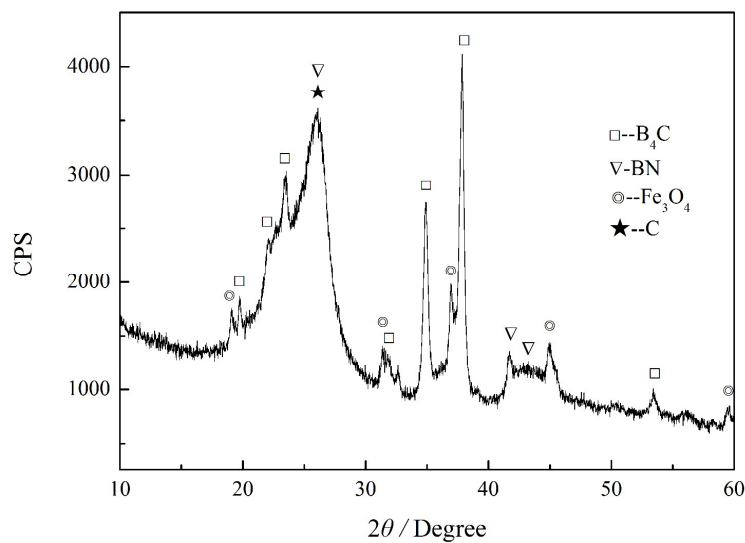
It can be seen from Figure 6 that there are no diffraction peaks of B_2O_3 , Mg and MgO, this is because B_2O_3 and MgO produced during the combustion are amorphous and there is little unreacted magnesium in the condensed phase products. Moreover, there is some $B_{12}Zr$, ZrO_2 and B_2Zr in the condensed phase products, and zirconium mainly comes from the impurity of boron powder.

#1 and #3 Sample were dissolved in the boiling dilute nitric acid first and then filtered with film of $0.45 \mu m$. XRD investigation of acid-insoluble substance (named

*1 and *3 respectively) was carried out and the results are shown in Figure 7.



(a) *1 sample



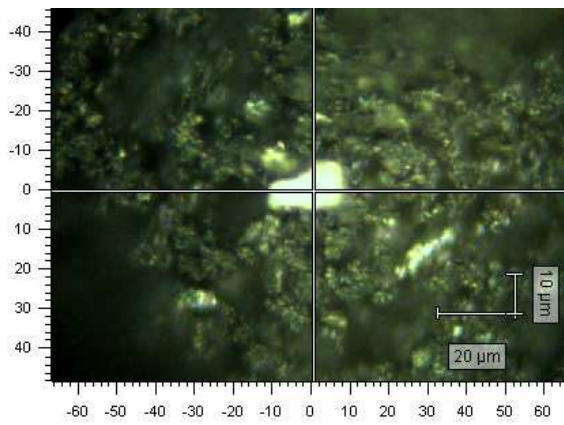
(b) *3 sample

Fig.7 XRD pattern of *1 and *3 sample

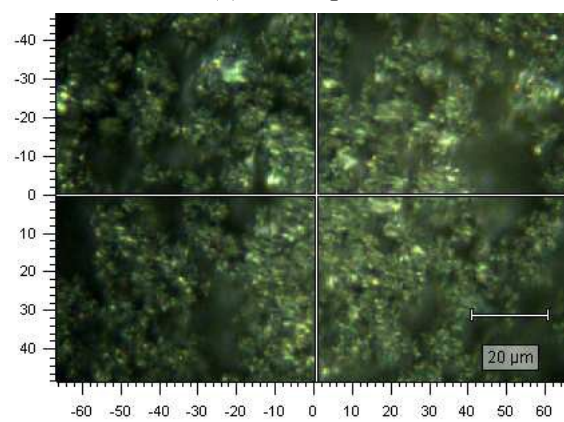
Figure 7 shows that the acid-insoluble substance is consisted of C, B_4C , (or $B_{12}C_2$), BN and Fe_3O_4 . BN produced under low pressure is amorphous basically, and BN produced under high pressure may be consisted of amorphous BN and *h*-BN.

*1 and *3 sample were also analyzed by Laser Raman Spectrometer (Renishaw, inVia Reflex) with laser of 532 nm wavelength excitation. Micrographs of the samples show

that there are marked bright zone and dark zone for *1 sample (Figure 8(a)), but no marked bright zone for *3 sample (Figure 8(b)).



(a) *1 sample



(b) *3 sample

Fig.8 Micrographs of the samples

Raman spectrum of the samples is shown in Figure 9.

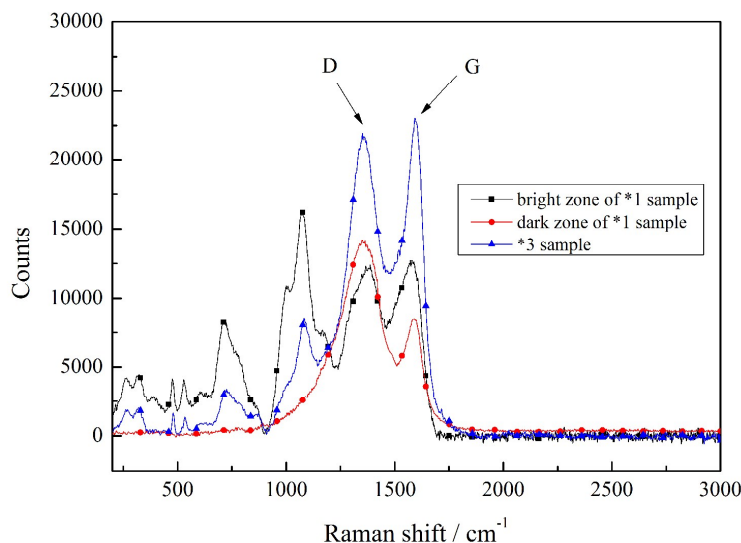


Fig.9 Raman spectrum of the samples

Figure 9 shows that the bright zone of *1 sample is mainly consisted of boron carbide and carbon, but only carbon in the dark zone¹⁹. This indicates that the bright zone (about 20 micros) is probably boron carbide, and the Raman shift of carbon may be result from the backdrop of carbon. *1 sample is mainly consisted of boron carbide and carbon, and there is no marked bright zone because the particle size of boron carbide produced in high pressure is very small.

So the dark zone of the samples is carbon, and from the intensity of D peak and G peak of carbon (I_D/I_G), the conclusion could be made that the higher chamber pressure, the higher graphitization degree of carbon²⁰.

3.2 Chemical analysis of condensed phase products quantitative aspect

XRD pattern results and thermodynamic calculation results indicate that the primary condensed phase products are mainly consisted of B, B₂O₃, C, B₄C, (or B₁₂C₂), BN, Mg, MgO, MgAl₂O₄, Al, Al₂O₃, AlCl₃, NH₄[Mg(H₂O)₆]Cl₃, NH₄Cl, Fe₃O₄ and small

amount of zirconium compound. As the content of zirconium in the propellant is less than 0.5 % (estimated by the purity of boron powder), zirconium compound in the primary condensed phase products could be neglected. The quantitative analysis scheme of condensed phase products is shown in Figure 10.

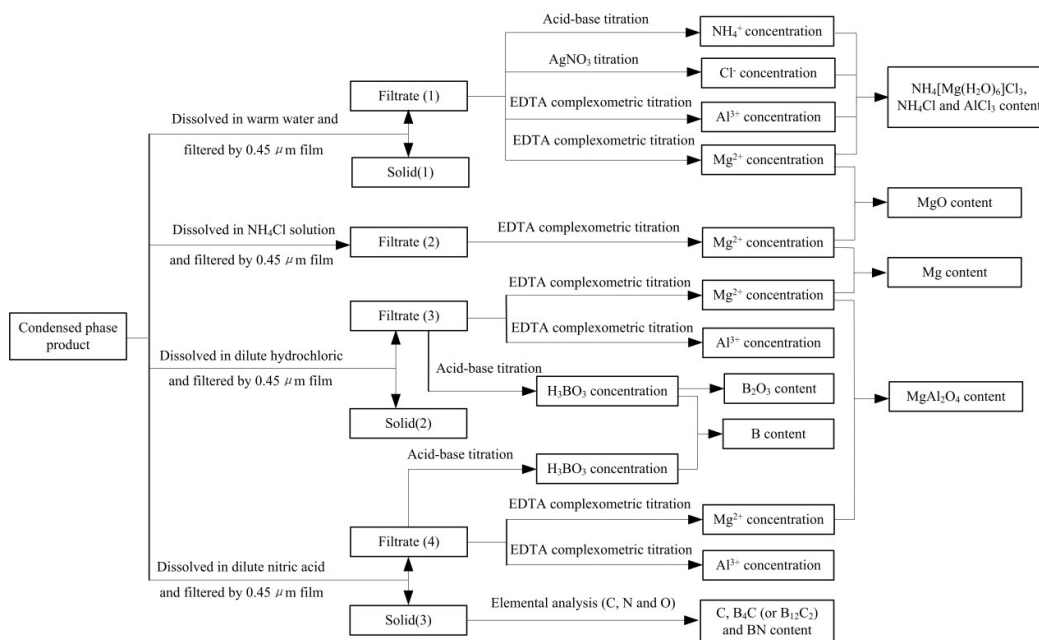


Fig.10 Quantitative analysis scheme of primary condensed phase products

The collected condensed phase products were dissolved in warm water and the content of $\text{NH}_4[\text{Mg}(\text{H}_2\text{O})_6]\text{Cl}_3$, NH_4Cl and AlCl_3 could be determined by the concentration of NH_4^+ , Cl^- , Mg^{2+} and Al^{3+} in the filtrate (1). Concentration of NH_4^+ was determined by acid-base titration with formaldehyde²¹, concentration of Cl^- was determined by precipitation titration and concentration of Mg^{2+} and Al^{3+} was determined by EDTA complexometric titration with xylenol orange and erichrome black T as indicator respectively.

Magnesium oxide could be dissolved in ammonium water solution, and the collected condensed phase products were dissolved in NH_4Cl water solution and the content of magnesium oxide could be determined by the concentration of Mg^{2+} in the filtrate (2) and the content of $\text{NH}_4[\text{Mg}(\text{H}_2\text{O})_6]\text{Cl}_3$ in the condensed phase products.

Collected condensed phase products were dissolved in dilute hydrochloric acid, the content of magnesium could be determined by the concentration of Mg^{2+} in the filtrate (3) and in the filtrate (1). The content of B_2O_3 was determined by concentration of H_3BO_3 in the filtrate (3), and concentration of H_3BO_3 could be determined by acid-base titration with mannitol. Moreover, the content of aluminum and aluminum oxide could be estimated roughly by the concentration of Al^{3+} in the filtrate (3) combined with the mass of solid (1) and solid (2).

Collected condensed phase products were dissolved in dilute nitric acid, the content of magnesia-alumina spinel (MgAl_2O_4) could be determined by the concentration of Mg^{2+} or Al^{3+} in the filtrate (4) and in the filtrate (3). The content of B_2O_3 was determined by concentration of H_3BO_3 in the filtrate (3) and filtrate (4).

So the content of B_2O_3 , B, MgO , Mg, MgAl_2O_4 , AlCl_3 , NH_4Cl and $\text{NH}_4[\text{Mg}(\text{H}_2\text{O})_6]\text{Cl}_3$ in the condensed phase products could be determined by the wet chemical analysis, the results are shown in Table 3.

Table 3 Results of wet chemical analysis

Sa mp le	B ₂ O ₃ / %	B /%	MgO/ %	Mg/ %	MgAl ₂ O ₄ /%	AlCl ₃ / %	NH ₄ Cl /%	NH ₄ [Mg(H ₂ O) ₆] Cl ₃ /%
#1	18.90	14.40	9.65	2.02	10.30	<0.01	4.64	3.68
#2	14.78	9.71	11.86	1.53	5.90	<0.01	4.53	3.67
#3	19.16	1.29	10.94	2.45	3.40	<0.01	5.01	0.05

Table 3 shows that the condensed phase products contain high amounts of B₂O₃ which indicates the high reactivity between oxygen and elemental boron during the primary combustion process and this would result in higher heat release during the primary combustion process due to the high heat of combustion of boron.

Table 3 also suggests that the content of elemental boron decreases evidently with the increase of chamber pressure but the content of boron oxide do not increase simultaneously which indicates that more the other boride was produced with the increase of chamber pressure. Also, there is little AlCl₃ in the primary condensed phase products and can be neglected in fact.

The results of XRD pattern indicates solid (3) is consisted of C, B₄C (or B₁₂C₂), BN and Fe₃O₄, and the content of those substances in the condensed phase products could be obtained by the content of them in solid (3) and the mass-loss of the condensed phase products in dilute nitric acid. All the ferrum in the combustion products should exist in the form of Fe₃O₄ because filtrate (3) is colorless, so the content of Fe₃O₄ could be obtained by the mass conservation of ferrum. Carbon is insoluble in acid and alkali and the level of carbon is usually measured by the high-temperature induction furnace method²², but there is boron carbide in solid (3) and boron carbide could also

be oxidized under oxygen environment at high temperature.

The mass-loss of B₄C (99 %, Aladdin Industrial Corporation) was measured by TGA (METTLER TOLEDO TGA/DSC 1) under a static atmosphere of oxygen (the flow rate of the sweeping gas is 30 ml/min), the sample weighing about 3 mg was heated at the rate of 5 °C/min from 300 °C to 900 °C, and alumina crucible was used to hold the sample. The result is shown in Figure 11.

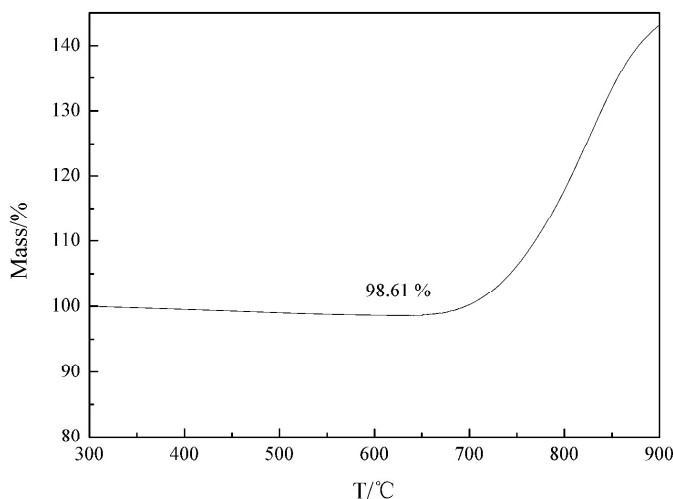


Fig. 11 TGA curve of B₄C

Figure 11 shows that the mass of B₄C begin to increase slowly when the temperature reaches as high as 640°C which indicates B₄C could be oxidized at the temperature more than 640°C. So the temperature must be controlled within 640°C when the high-temperature induction furnace method was used to determine the content of carbon.

TGA experiments were carried out for solid (3) of different condensed phase products (named *1, *2 and *3 respectively) under a static atmosphere of oxygen, the sample

weighing about 3 mg was heated at 600°C for 40 minutes, and alumina crucible was used to hold the sample. The results are shown in Figure 12.

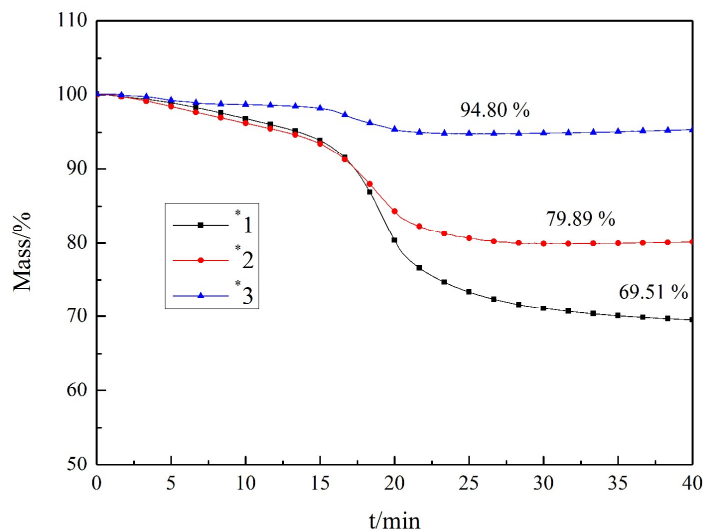


Fig.12 TGA curves of solid (3)

Figure 12 shows that the maximum mass-loss of samples is different. Assume that all the carbon was oxidized and the mass-loss results from the oxidation of carbon, the content of carbon in different condensed phase products could be determined by the maximum mass-loss of samples and the mass-loss of samples in dilute nitric acid.

The results suggest that the content of carbon in #1, #2 and #3 samples is 9.6 %, 5.2 % and 2.6 % respectively. As the system is fuel-rich, large amounts of carbon should be produced during the primary combustion of boron-based fuel-rich propellant, so the results of TGA may be deviate from the fact value. The graphitization degree of carbon produced under low pressure is lower than that produced under high pressure. The carbon with higher graphitization degree reacts with oxygen more difficultly and the oxidation process is not complete under the experimental conditions.

Boron carbide and boron nitride are all stable substance, and the content of them is difficult to be determined^{23,24}. Therefore, the content of elements carbon, oxygen and nitrogen in solid (3) was measured by element analyzer (LECO CS600 and LECO TC-436), and then the content of carbon, boron carbide and boron nitride could be obtained.

Table 4 Results of elementary analysis

Sample	C/%	N/%	O/%
*1	37.93	6.57	2.77
*2	39.05	5.60	1.52
*3	36.13	5.68	1.25

The content of Fe_3O_4 in solid (3) could be determined by the mass conservation of ferrum, but the content of oxygen in solid (3) calculated by Fe_3O_4 (1.53 %, 1.14 % and 0.98 %) is higher than the experimental value which suggests that there is small amount of the other oxides in solid (3). As the amount of these oxides is very low, the content of them can be neglected. But in order to make the results more accurate, experimental oxygen content and calculated ferrum content were used in the chemical analysis of solid (3). So the content of element boron in solid (3) could be determined by

$$\omega_B = 1 - \omega_C - \omega_N - \omega_{Fe} - \omega_O$$

where ω_C , ω_N , ω_{Fe} and ω_O are the content of element carbon, nitrogen, ferrum and oxygen in solid (3) respectively.

The content of boron nitride in solid (3) could be determined by content of element

nitrogen directly. Element boron exists in the form of boron carbide and boron nitride, so the content of boron carbide (B_4C or $B_{12}C_2$) in solid (3) could be calculated by the mass conservation of element boron and the content of boron nitride. Boron exists in the form of boron carbide and carbon, so the content of carbon in solid (3) could be calculated by the mass conservation of carbon and the content of boron carbide. Then the content of carbon, boron carbide and boron nitride could be obtained by the mass-loss of the condensed phase products in the dilute nitric acid (68.37 %, 57.45 % and 50.15 % respectively), the results are shown in Table 5.

Table 5 Content of the other substances in condensed phase products

Sample	C/%	B_4C /%	$B_{12}C_2$ /%	BN/%
*1	15.99	-	12.37	3.68
*2	13.28	25.30	-	4.22
*3	11.01	32.22	-	4.72

It can be seen from Table 5 that large amounts of boron carbide are generated during the primary combustion of boron-based fuel-rich propellant, and the content of boron carbide seems to increase with the chamber pressure. The results also explain why the content of elemental boron decreases obviously but the content of boron oxide does not increase simultaneously with the increase of chamber pressure.

In addition, the content of carbon in *1 sample is almost the same as the one calculated by TGA results but it is not the case for the other samples which validates the conclusion that carbon of high graphitization degree is produced under high pressure.

Table 5 also shows that a small amount of boron nitride is produced during the primary combustion and it seems that the content of boron nitride increases slightly with chamber pressure.

3.3 Calculation of the percentage of gaseous products

The percentage of gaseous products (PGP) is an important parameter of fuel-rich propellant, could not only provide a parameter to estimate the combustion performance of the fuel-rich propellant but also yield experimental data for comparison with the results of thermodynamic calculation²⁵.

Although chemical analysis was carried out with the condensed phase products in section 3.2, but the aim of this research is to obtain the content of the products in the total combustion products. As the total mass of condensed phase products or gaseous products could not be obtained accurately, converting the results of the chemical analysis by a conversion factor may be a good choice. PGP refers to the mass ratio of the gaseous products to the total products, and could be regarded as the conversion factor.

Considering that all the magnesium and aluminum in condensed phase products is dissolved in dilute nitric acid and the content of magnesium and aluminum in the propellant is known, PGP value could be determined accurately by the mass conversation of magnesium or aluminum.

Take the mass conversation of magnesium for example. Assuming that condensed

phase products weighing m_s is dissolved in boiling dilute acid, and the number of moles of Mg^{2+} in filtrate is $n_{Mg^{2+}}$, thus the percentage of magnesium in condensed phase products φ_{Mg} is:

$$\varphi_{Mg} = \frac{n_{Mg^{2+}} \cdot M_{Mg}}{m_s} \quad (1)$$

where M_{Mg} is the atomic mass of magnesium. If the content of magnesium in the propellant is ω_{Mg} , the mass conversation of magnesium could be expressed as follow:

$$(1 - \eta_0) \omega_{Mg} = \varphi_{Mg} \quad (2)$$

where η_0 is the PGP of the experiment. So the PGP of the experiment could be determined as follow:

$$\eta_0 = 1 - \frac{\omega_{Mg}}{\varphi_{Mg}} = 1 - \frac{\omega_{Mg} \cdot m_s}{n_{Mg^{2+}} \cdot M_{Mg}} \quad (3)$$

There are $NH_4[Mg(H_2O)_6]Cl_3$ and NH_4Cl in the collected condensed phase products and they are produced by reactions among NH_3 , HCl , $MgCl_2$ and H_2O . $NH_4[Mg(H_2O)_6]Cl_3$ and NH_4Cl should exist in the form of gaseous products if the combustion products is not cooled to the room temperature, so the PGP value obtained from Eq.(3) is only the nominal PGP value. Then the content of condensed phase products in combustion products could be obtained by the content of them in collected condensed phase products and the nominal PGP value(29.89 %, 30.40 % and 27.51 % respectively), and the results are shown in Table 6.

Table 6 Contents of some important substances in combustion products

NO.	B/%	B ₂ O ₃ /%	B ₁₂ C ₂ /%	B ₄ C/%	BN/%	C/%
1	10.10	13.25	11.47	-	2.58	11.21
2	6.76	10.29	-	17.61	2.94	9.24
3	0.93	13.90	-	23.36	3.42	7.98

Table 6 shows that the mass ratio of the substances in combustion products is basically consistent with the one in condensed phase products. There is a large amount of boron carbide in the primary combustion products of boron-based fuel rich propellant especially under high pressure which may be not disadvantageous to the heat release of secondary combustion because of its high stability²⁶.

In addition, the real PGP value could be obtained by the adjustment of the nominal one. Assuming that the content of NH₄[Mg(H₂O)₆]Cl₃ and NH₄Cl in the condensed phase products is φ_{NMHCl} and φ_{NH_4Cl} , then the nominal percentage of NH₄[Mg(H₂O)₆]Cl₃ and NH₄Cl in the combustion products is

$$\psi_{NMHCl} = \varphi_{NMHCl}(1 - \eta_0)$$

$$\psi_{NH_4Cl} = \varphi_{NH_4Cl}(1 - \eta_0)$$

so the adjusted PGP η could be expressed by:

$$\eta = \eta_0 + \psi_{NMHCl} + \psi_{NH_4Cl} \quad (4)$$

The real PGP values of three experiments could be calculated from Eq.(4), and are 38.21 %, 38.60 % and 32.60 % respectively. Similarly, the PGP value also could be

determined by the mass conservation of aluminum.

4 Preliminary analysis of the organics and gases products in the primary combustion products

There is some oil-like organics floating on the solution when the condensed phase products are dissolved in different solutions, and it seems that the content of organics decreases with the increase of chamber pressure. The primary combustion temperature of boron-based fuel-rich propellant is much lower than the regular composite propellant because of low content of oxidizer, so the binder of propellant may be not combust completely and some organics are produced during the combustion process.

These organics are also the components of condensed phase products, but they cannot be determined by titration. The condensed phase products were dissolved in acetone, and the filtrate (named &1, &2 and &3 respectively) was analyzed by using Fourier Transform Infrared Spectrometer (Bruker Tensor 27). The results are shown in Figure 13.

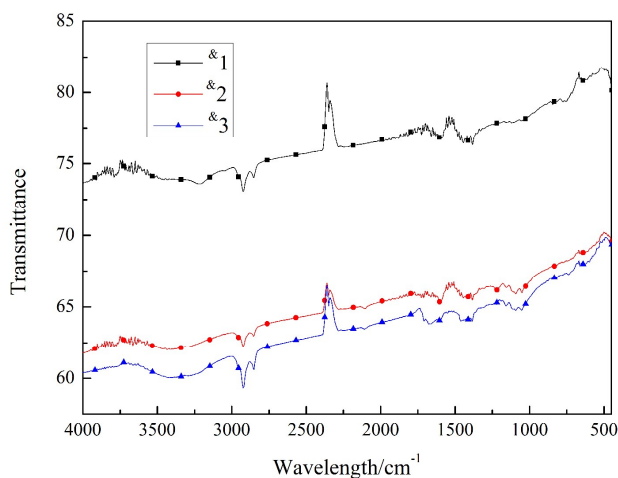


Fig.13 FTIR spectrum

Figure 13 indicates that the organics in different combustion products are almost the same and may be one substance. According to the characterizing absorption bands of chemical groups, the organics could be characterized by cycloalkanes (2924 cm^{-1} , 2854 cm^{-1} , 1655 cm^{-1} and 1465 cm^{-1}) and alcohol (3400 cm^{-1} and 1400 cm^{-1}). From the ingredients of boron-based fuel-rich propellant, the organics should come from the unoxidized (or partially oxidized) decomposition products of binder (HTPB).

There are many decomposition products of HTPB²⁷, such as butadiene, 4-vinylcyclohexene, ethylene, cyclopentene, 1,5-hexadiene and trans-butadiene oligomers. The main species are butadiene monomer, 4-vinylcyclohexene and trans-butadiene oligomers, but the boiling point of butadiene is very low and cannot exist in the condensed phase products. So the organic could be cyclohexaneethanol according to the FTIR spectrum and produced from the partially oxidized 4-vinylcyclohexene.

The collected gases products (named $\hat{1}$, $\hat{2}$ and $\hat{3}$ respectively) were analyzed by FTIR (Bruker, Tensor27) with the gas cell of 2.4 meters length. The wavelength is from 4000 to 400 cm^{-1} and the resolution is 0.5 cm^{-1} . The infrared spectrum of three samples is almost the same and one of them is shown in Figure 14.

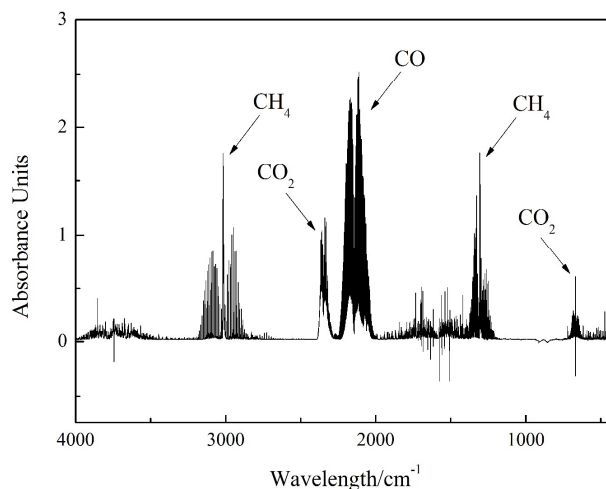


Fig.14 FTIR spectrum of the gas products

Figure 14 shows that there are mainly CH₄, CO and CO₂ in the gas products. In order to analyze the gas products quantitatively, gas chromatography (Agilent GC-6820) with argon as carrier gas and thermal conductivity detector (TCD) was employed to determine the composition of the three gas samples. Two packed columns (propark Q and 13 X molecular sieves) were used to separate gases. The gas samples were separated first by columns of propark Q, and the results show that there is no CO₂ in the three gas samples. Then the gas samples were separated by columns connected in a series, and the results show that all the gas samples are mainly consisted of H₂, N₂, CH₄ and CO.

The content of gases was quantified by external standard, and the results are shown in Table 7.

Table 7 Component of gases products

Sample	H ₂ /%	N ₂ /%	CH ₄ /%	CO/%
[^] 1	25.04	9.87	2.13	15.70
[^] 2	25.50	9.76	2.08	2.59
[^] 3	25.29	10.92	2.04	1.07

Table 7 suggest that a large amount of H₂ produced during the combustion process which is benefit for the ejection efficiency of the primary condensed products and heat release of the secondary combustion because of the low molecular weight and high combustion heat of H₂.

Considerable quantities of CO are produced in low chamber pressure and the content of CO decreases obviously with the increase of chamber pressure. From the composition of the combustion products, carbon element exists mainly in the form of born carbide, carbon and carbon monoxide at low chamber pressure while born carbide and carbon at high chamber pressure. Born carbide is produced by the reactions of elemental boron and hydrocarbon (CH₄, C₂H₄, C₄H₆, etc.), so the decrease of CO may be result from the higher reaction ability of elemental boron and hydrocarbon.

It's should be noted that the combustion products were cooled with argon in this study, and then there is large amount of argon in the collected gaseous products. However, argon in the gas samples cannot be detected by TCD during the GC experiments because argon was employed as carrier gas which results in the total four gases content in Table 7 is far below 100 %.

5 Conclusions

(1) A test facility was designed to collect the primary combustion products of boron-based fuel-rich propellants under different pressures, and the chemical analysis was carried out for almost all the combustion products (condensed phase products and

gases products) with different methods.

(2) There are large amounts of boron oxide and boron carbide in the condensed phase products which indicates that elemental boron is highly active during the primary combustion process. The content of elemental boron decreases obviously with the increase of chamber pressure, and this is mainly due to the production of boron carbide.

(3) Chamber pressure is an important parameter and plays two different roles in the secondary combustion of boron-based fuel-rich propellants, the first is when the particle size of condensed phase fuels decreases with the increase of pressure which results in higher combustion efficiency directly, the second is when more boron carbide, graphite and *h*-BN (especially boron carbide) are produced under higher pressure which is unfavorable to the combustion efficiency.

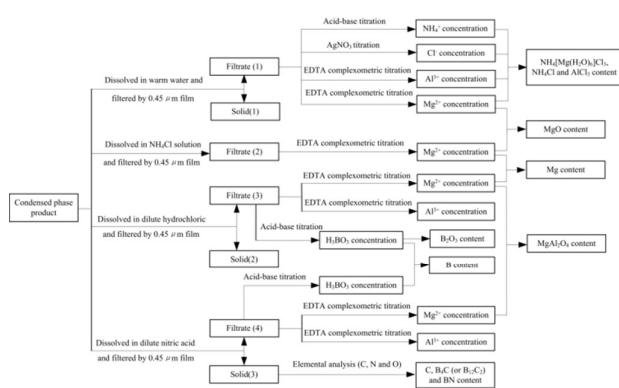
Acknowledgement

This research is supported by the Key Foundation of Science and Technology on Combustion, Internal Flow and Thermal-Structure Laboratory (9140C520102150C52009).

References

1. K. K. Kuo and M. Summerfield, *Fundamentals of solid-propellant combustion*, American Institute of Aeronautics and Astronautics, 1984.
2. H. Books, *Rocket Propellants, Including: Aluminium, Boron, Ethanol, Gunpowder, Liquid Hydrogen, Hydrazine, Hypergolic Propellant, Unsymmetrical Dimethylhydrazine, Diborane, Nitromethane, Monomethylhydrazine, C-Stoff, Hydroxylamine, Rp-1, Aerozine 50, Decaborane*, Hephaestus Books, 2011.
3. A. Gany and Y. M. Timnat, *Acta Astronautica*, 1993, **29**, 181-187.

4. H. Besser and R. Strecker, *Combustion of boron-based solid propellants and solid fuels*(A 95-11126 01-28), Boca Raton, FL, CRC Press, Inc., 1993, 1993, 133-178.
5. R. S. Fry, *J Propul Power*, 2004, **20**, 27-58.
6. C. Vigot, A. Cochet and C. Guin, *International Journal of Energetic Materials and Chemical Propulsion*, 1993, **2**.
7. K. Schadow, *Combust Sci Technol*, 1972, **5**, 107-117.
8. B. Hussmann and M. Pfitzner, *Combust Flame*, 2010, **157**, 803-821.
9. B. Hussmann and M. Pfitzner, *Combust Flame*, 2010, **157**, 822-833.
10. D. Cruise, *Theoretical Computations of Equilibrium Compositions, Thermodynamic Properties, and Performance Characteristics of Propellant Systems*, DTIC Document, 1979.
11. R. Gautam and W. D. Seider, *AIChE Journal*, 1979, **25**, 991-999.
12. N. S. Cohen, *Aiaa J*, 1969, **7**, 1345-1352.
13. T. Mitani and M. IZUMIKAWA, *J Spacecraft Rockets*, 1991, **28**, 79-84.
14. R. Pein and F. Vinnemeier, *J Propul Power*, 1992, **8**, 609-614.
15. R. Pein, H. Ciezki and A. Eicke, 1995.
16. H. Blumenthal, *Anal Chem*, 1951, **23**, 992-994.
17. J. Willis, *Anal Chem*, 1961, **33**, 556-559.
18. R. bin Othman, J. O. Hill and R. J. Magee, *Microchimica Acta*, 1986, **90**, 337-350.
19. T. L. Aselage, D. R. Tallant and D. Emin, *Phys Rev B*, 1997, **56**, 3122-3129.
20. M. B. Vazquez-Santos, E. Geissler, K. Laszlo, J. N. Rouzaud, A. Martinez-Alonso and J. M. D. Tascon, *J Phys Chem C*, 2012, **116**, 257-268.
21. B. Karlmark, *Analytical biochemistry*, 1973, **52**, 69-82.
22. D. W. Nelson, L. E. Sommers, D. Sparks, A. Page, P. Helmke, R. Loeppert, P. Soltanpour, M. Tabatabai, C. Johnston and M. Sumner, *Methods of soil analysis. Part 3-chemical methods.*, 1996, 961-1010.
23. M. Bouchacourt and F. Thevenot, *Journal of materials science*, 1985, **20**, 1237-1247.
24. W. Gruner, J. Haßler, P. Barth, J. Behm and J. Sunderkötter, *Journal of the European Ceramic Society*, 2009, **29**, 2029-2035.
25. L.-L. Liu, G.-Q. He and Y.-H. Wang, *Hanneng Cailiao(Chinese Journal of Energetic Materials)*, 2012, **20**, 475-478.
26. J. A. Nabity, T.-H. Lee, B. Natan and D. W. Netzer, *International Journal of Energetic Materials and Chemical Propulsion*, 1993, **2**.
27. T. Brill and B. Budenz, *Solid propellant chemistry, combustion, and motor interior ballistics, volume 185*, 2000, **185**, 1.



The content of solid primary products of boron-based fuel-rich propellants could be determined quantitatively through the analysis procedure.